

Phase Shifters With Wide Range of Phase and Ultra-Wideband Performance Using Stub-Loaded Coupled Structure

L. Guo and A. Abbosh, *Senior Member, IEEE*

Abstract—Compact planar phase shifters with wide range of differential phase shift across ultra-wideband frequency are proposed. To achieve that performance, the devices use broadside coupled structure terminated with open-ended or short-ended stubs. The theory of operation for the proposed devices is derived. To validate the theory, several phase shifters are designed to achieve a differential phase ranging from -180° to 180° . Moreover, three prototypes are developed and tested. The simulated and measured results agree well with the theory and show less than 7° phase deviation and 1.4 dB insertion loss across the band 3.1–10.6 GHz.

Index Terms—Coupler, phase shifter, ultra-wideband (UWB).

I. INTRODUCTION

PHASE shifters are widely used in many microwave systems, such as phased arrays, modulators, microwave instrumentation and measurement systems. Different techniques are used to build planar phase shifters with wideband performance, such as broadside-coupled structure [1]–[4], modified Schiffman [5], composite right/left-handed transmission lines [6], loaded transmission lines [7], substrate integrated waveguide [8]–[10], double microstrip-slot transitions [11], or metamaterials [12].

A careful inspection of the performance of the developed phase shifters indicates that only a few of them cover the ultra-wideband (UWB) frequency range (3.1–10.6 GHz) [1]–[4], [7], [11]. Despite their excellent performances across almost the whole UWB range, one section of those devices can achieve a maximum phase shifts of 45° [1]–[3], or 90° [4], [7], [11]. Thus, to achieve wider phase ranges, multiple sections of those devices are to be cascaded. That approach causes an increase in the phase deviation, insertion loss, and size.

Compact UWB phase shifters with wide range of phase shifts (from -180° to $+180^\circ$) using a single coupled structure is presented. The proposed design is a modification of [1]. A recent modification of [1] extends the phase range to 90° on a cost of increased insertion loss and reduced bandwidth [4]. To dramatically increase the phase range by several times without negative impacts on the performance, two short-ended or open-ended

stubs are properly designed and connected to the coupled microstrip patches. The presented design is supported via theory, simulations and measurements.

II. THEORY

The proposed phase shifter is shown in Fig. 1. It uses two broadside-coupled microstrip patches at the top and bottom layer of a multilayer structure. One terminal of each of those patches is connected to the input or output feeder, whereas the other terminal is connected to an open- or short-ended stub. The ground plane is located in the central layer that separates the coupled patches. A slot is created at the ground plane to control the coupling between the top and bottom layers.

The coupling factor of the coupled structure and dimensions of the utilized stubs are used to control the phase of a microwave signal passing through the proposed configuration. The structure in Fig. 1 can be analyzed using the even-odd mode approach [1]. To include the effect of the stubs, the transmission line theory is also used. To that end, it is possible to show that the S-parameters of the device are

$$S_{11} = \frac{1 - C^2(1 + \sin^2(\beta_{ef}l))\Gamma_{\text{open, short}}}{[\sqrt{1 - C^2} \cos(\beta_{ef}l) + j \sin(\beta_{ef}l)]^2} \quad (1)$$

$$S_{21} = \frac{j2C\sqrt{1 - C^2} \sin(\beta_{ef}l)\Gamma_{\text{open, short}}}{[\sqrt{1 - C^2} \cos(\beta_{ef}l) + j \sin(\beta_{ef}l)]^2} \quad (2)$$

$$\Gamma_{\text{open}} = \frac{jZ_{\text{st}} \cot(\beta_{\text{st}}l_{\text{st}}) + Z_{\text{cl}}}{jZ_{\text{st}} \cot(\beta_{\text{st}}l_{\text{st}}) - Z_{\text{cl}}};$$

$$\Gamma_{\text{short}} = \frac{jZ_{\text{st}} \tan(\beta_{\text{st}}l_{\text{st}}) - Z_{\text{cl}}}{jZ_{\text{st}} \tan(\beta_{\text{st}}l_{\text{st}}) + Z_{\text{cl}}} \quad (3)$$

C : coupling factor, which is controlled by the width of the patch at the top and bottom layers (D_m), and width of the slot at the middle layer (D_s) [13]–[15], Z_{cl} : characteristic impedance of the coupled line defined by the required coupling factor [13], [15], Z_{st} : characteristic impedance of the open-ended (or short-ended) stubs, β_{st} and l_{st} : phase constant and length of the open-ended (or short-ended) stubs, respectively, l : length of the coupled line, Γ : reflection coefficient of the open-ended or short-ended stubs, ϵ_r : dielectric constant of the substrate, λ : free-space wavelength, β_{ef} : effective phase constant in the medium of the coupled structure.

To obtain a certain differential phase shift, a comparison is made with a reference transmission line of 50Ω impedance, physical length l_m and phase constant β_m . Therefore, the differential phase shift $\Delta\phi$ of the coupled structure with open-ended

Manuscript received August 01, 2013; revised October 30, 2013; accepted November 23, 2013. Date of publication January 13, 2014; date of current version March 07, 2014. This work was supported by the Australian Research Council, Discovery Grant DP120101214.

The authors are with the School of ITEE, The University of Queensland, Brisbane, St. Lucia QLD 4072, Australia (e-mail: l.guo3@uq.edu.au).

Color versions of one or more of the figures in this paper are available online at <http://ieeexplore.ieee.org>.

Digital Object Identifier 10.1109/LMWC.2013.2293658

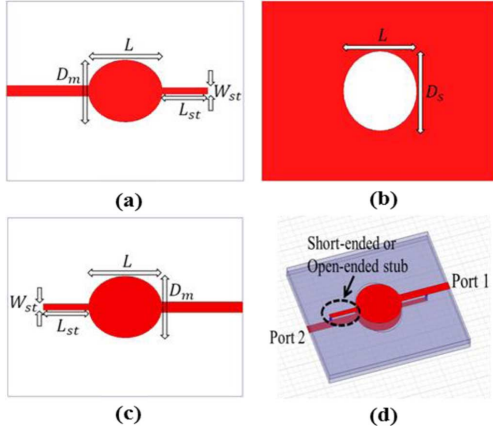


Fig. 1. Configuration of the proposed phase shifter. (a) Top layer, (b) middle layer, (c) bottom layer, and (d) whole structure.

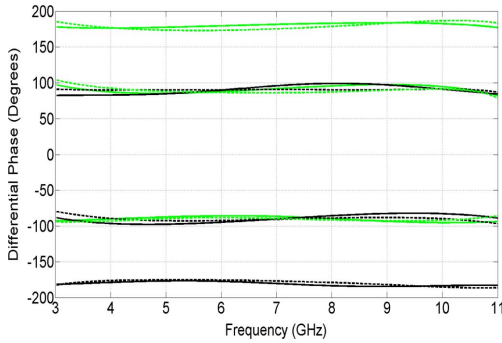


Fig. 2. Theoretical and simulated phase shifts. Black lines: devices with short-ended stubs, green lines: devices with open-ended stubs. Solid-lines: theory, dash-lines: simulations.

TABLE I
CALCULATED AND OPTIMIZED DESIGN PARAMETERS

Parameter (ohm or mm)		Z_{st}	W_{st}	L_{st}	L	D_m	D_s
-180° open-ended stub	Cal	117	0.2	5.9	7.2	5.1	7.3
	Opt	117	0.2	6.3	7.3	4.7	7.6
-90° open-ended stub	Cal	23	3.5	5.2	7.2	4.3	9.2
	Opt	23	3.5	5.2	8.4	3.7	10.9
-90° short-ended stub	Cal	26	3	4.8	7.2	6.1	7.4
	Opt	28	2.7	4.8	7.1	5.8	6.7
90° open-ended stub	Cal	100	0.3	5.4	7.2	4.6	6.5
	Opt	89	0.4	5.9	7.5	3.2	5.9
90° short-ended stub	Cal	117	0.2	5.8	7.2	6.1	8.2
	Opt	117	0.2	6.7	7.2	7.9	9.1
180° short-ended stub	Cal	56	1	5.4	7.2	6.1	8.2
	Opt	68	0.7	4.8	7.8	6.9	8.9

or short ended stubs can be calculated from (1)–(3). For a structure using certain stubs' type, the relevant reflection coefficient is substituted from (3) in (2). The phase of (S_{21}) is then calculated from the resultant equation as follows:

$$\Delta\Phi_{\text{open}} = -90^\circ + 2 \arctan \left[\frac{Z_{st} \cot(\beta_{st} l_{st})}{Z_{cl}} \right] - 2 \arctan \left[\frac{\sin(\beta_{ef} l)}{\sqrt{1 - C^2} \cos(\beta_{ef} l)} \right] + \beta_m l_m \quad (4)$$

$$\Delta\Phi_{\text{short}} = -90^\circ - 2 \arctan \left[\frac{Z_{st} \tan(\beta_{st} l_{st})}{Z_{cl}} \right] - 2 \arctan \left[\frac{\sin(\beta_{ef} l)}{\sqrt{1 - C^2} \cos(\beta_{ef} l)} \right] + \beta_m l_m. \quad (5)$$

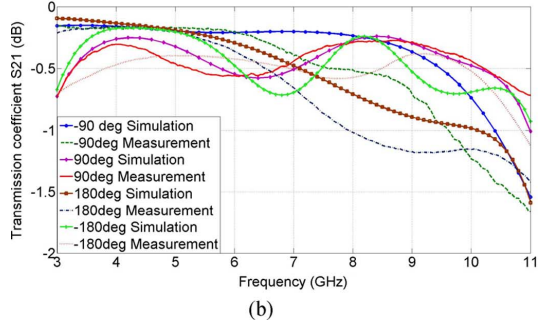
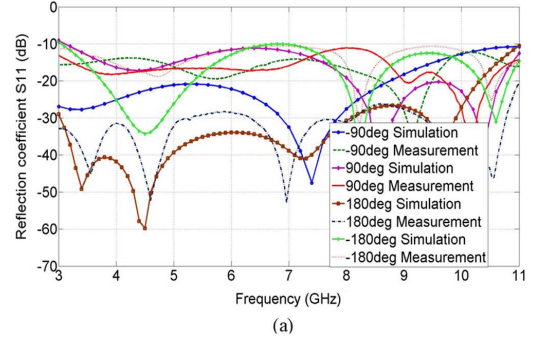


Fig. 3. Reflection (a) and transmission (b) coefficients of the devices.

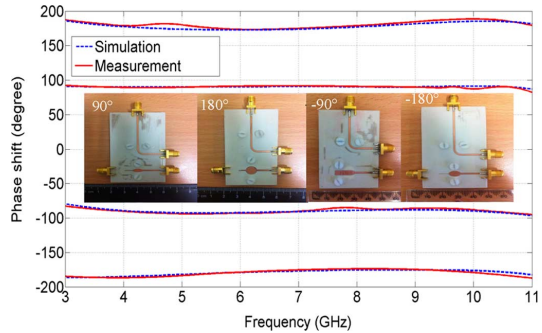


Fig. 4. Simulated and measured differential phase shift for the four developed phase shifters (shown in inset).

TABLE II
COMPARISON BETWEEN RECENT UWB PHASE SHIFTERS

Ref#	Max. phase range	Phase deviation	Trans coeff. (dB)	Size (wavelengths)
[1]	45°	3°	-1.3	0.2 × 0.25
[2]	45°	5°	-1	0.15 × 0.55
[3]	45°	3°	-0.4	0.2 × 0.6
[4]	90°	8°	-2.3	0.15 × 0.75
[6]	45°	5°	-1	0.25 × 0.3
[7]	90°	9°	-1	0.54 × 0.81
[11]	90°	8°	-1.8	0.25 × 0.25
This work	270°	7°	-1.4	0.2 × 0.45

For a characteristic impedance of 50Ω for the coupled lines, (4) and (5) indicate that the differential phase shift can be controlled by the length l_{st} and width w_{st} of the stubs (calculated from the stub's impedance using the well-known microstrip equations) and the coupling factor.

To investigate the effect of different design parameters on the differential phase, the derived (1)–(5) are included in a parametric study in Matlab. In that study, the conditions for an acceptable design were set at less than 1 dB of insertion loss and more than 10 dB of return loss across the band 3.1–10.6 GHz. To meet those design requirements, the parametric study shows that the coupling factor should be between

0.7 and 0.8, whereas the coupling length should be a quarter of the effective wavelength. According to that study, it was found that a single-section phase shifter with open-ended stubs can achieve any phase shift from -180° to $+90^\circ$, whereas the device with short-ended stubs can achieve a phase shift from -90° to $+180^\circ$. Snapshots of the results from (1)–(5) showing achieved phase shifts of -180° , -90° , 90° , and 180° phase shifts are shown in Fig. 2. The coupling factor needed to realize -90° , 90° , and 180° phase shifts is 0.78, whereas a coupling of 0.72 was needed to achieve 180° phase shift. The dimensions of the stubs to achieve those phase values are calculated using (1)–(5) and listed in the first four columns of values in Table I. According to Fig. 2, the designed phase shifters have phase deviations from the nominal values of less than 6° across the UWB range (3.1–10.6 GHz).

III. SIMULATIONS AND MEASUREMENT

The full-wave electromagnetic simulator ANSYS HFSS is used to verify the theoretical results. The substrate selected for the devices is Rogers RO4003C, with dielectric constant $\epsilon_r = 3.38$ and thickness of 0.5 mm. The calculated coupling coefficients were used to find the even- and odd-mode impedances of the coupled lines (Z_{oe} , Z_{oo}) which were then used to find the dimension of the coupled lines (D_m and D_s) using the conformal mapping techniques described in [13]. All the calculated dimensions were optimized using the simulation tool HFSS. The calculated and optimized dimensions are shown in Table I, which indicates their close agreement.

The simulated differential phase shift ($\Delta\phi$), reflection coefficient (S_{11}) and transmission coefficient (S_{21}) of the designed devices are shown in Figs. 2 and 3. For the -180° , -90° , 90° and 180° phase shifters, the simulated deviations in the phase from the nominal value are 6° , 5° , 1° , and 6° , respectively, across the frequency band 3.1–10.6 GHz as depicted in Fig. 2. It is clear from the simulated results in Fig. 3(a) that the reflection coefficients for all the simulated devices are less than -10 dB across the frequency range 3–11 GHz. As depicted in Fig. 3(b), the transmission coefficients for the simulated devices are more than -0.7 dB, -1.2 dB, -0.6 dB, and -1.2 dB for the -180° , -90° , 90° , and 180° phase shifters, respectively, over the band 3.1–10.6 GHz.

To further prove the validity of the proposed design and to support the presented theory and simulations, the $\pm 90^\circ$ and $\pm 180^\circ$ phase shifters were manufactured and tested. To eliminate the effect of any air gap between the two substrates used to build any of the devices, plastic screws are used to fix and align those substrates. Sub-Miniature A (SMA) connectors were used to connect the devices to the test equipment. To enable connecting the SMAs with the middle-layer ground of the devices, a small part of the substrate was cut properly. The measured results are shown in Figs. 3 and 4. Those results support the derived theory and simulations and validate the design method. As depicted in Fig. 3(a), the reflection coefficients for those devices are less than -10 dB across the band 3–11 GHz. Fig. 3(b) indicate that the measured transmission coefficients are less than 0.7 dB, 1.4 dB, 0.6 dB, and 1.2 dB for the -180° , -90° , 90° and 180° phase shifters, respectively, across the band 3.1–10.6 GHz. The measured differential phases of the devices are equal to the nominated values with a phase deviation of less than 6° , 2° , 5° , and 7° for the developed -180° , -90° , 90° and 180° phase

shifters, respectively, over the frequency band 3.1–10.6 GHz. All the measured results agree well with the simulations.

A comparison between the proposed phase shifter and UWB phase shifters published in the last two years is presented in Table II. In the comparison, the phase range is the maximum possible value using one section with realizable dimensions. Also, the size (in effective wavelengths) is taken for one section and excludes the feeders and reference lines. Table II indicates that the presented devices have the widest coverage of differential phase using a compact structure. The phase stability, return loss and insertion loss are all reasonable for UWB applications.

IV. CONCLUSION

Planar phase shifters with wide differential phases across UWB frequency have been presented. The devices use broad-side multilayer coupled structures terminated with open-ended and short-ended stubs. The derived theory, simulations and measurements show the capabilities of the proposed devices to achieve phase shifts in the range from -180° to 90° when using short-ended stubs and from -90° to 180° with open-ended stubs. The results of four developed devices for phase shifts of -180° , -90° , 90° , and 180° indicate less than 7° phase deviation and 1.4 dB insertion loss across the band 3.1–10.6 GHz.

REFERENCES

- [1] A. Abbosh, "Ultra-wideband phase shifters," *IEEE Trans. Microw. Theory Tech.*, vol. 55, no. 9, pp. 1935–1941, Sep. 2007.
- [2] S. H. Yeung, K. F. Man, and W. S. Chan, "The multiple circular sectors structures for phase shifter designs," *IEEE Trans. Microw. Theory Tech.*, vol. 59, no. 2, pp. 278–285, Feb. 2011.
- [3] A. Abbosh, "Broadband fixed phase shifters," *IEEE Microw. Wireless Compon. Lett.*, vol. 21, no. 1, pp. 22–24, Jan. 2011.
- [4] M. Sorn, R. Lech, and J. Mazur, "Simulation and experiment of a compact wideband 90° differential phase shifter," *IEEE Trans. Microw. Theory Tech.*, vol. 60, no. 3, pp. 494–501, Mar. 2012.
- [5] Y. Guo, Z. Zhang, and L. Ong, "Improved wideband Schiffman phase shifter," *IEEE Trans. Microw. Theory Tech.*, vol. 54, no. 3, pp. 1196–1200, Mar. 2006.
- [6] H. Y. Zeng, G. M. Wang, Y. W. Wang, and X. J. Gao, "Ultra-wideband 45° phase shifter based on simplified composite right/left-handed transmission line," *Electron. Lett.*, vol. 48, no. 25, pp. 1608–1610, 2012.
- [7] S. H. Yeung, Z. Mei, T. K. Sarkar, and M. Salazar-Palma, "Design and testing of a single-layer microstrip ultrawideband 90° differential phase shifter," *IEEE Microw. Wireless Compon. Lett.*, vol. 23, no. 3, pp. 122–124, Mar. 2013.
- [8] T. Yang, M. Ettorre, and R. Sauleau, "Novel phase shifter design based on substrate integrated waveguide technology," *IEEE Microw. Wireless Compon. Lett.*, vol. 22, no. 10, pp. 518–520, Oct. 2012.
- [9] Y. Cheng, W. Hong, and K. Wu, "Broadband self-compensating phase shifter combining delay line and equal-length unequal-width phaser," *IEEE Trans. Microw. Theory Tech.*, vol. 58, no. 1, pp. 203–210, Jan. 2010.
- [10] O. Kramer, T. Djerfai, and K. Wu, "Dual-layered substrate-integrated waveguide six-port with wideband double-stub phase shifter," *IET Microw. Antennas Propag.*, vol. 6, no. 15, pp. 1704–1709, 2012.
- [11] Y. Wang, M. E. Bialkowski, and A. M. Abbosh, "Double microstrip-slot transitions for broadband $\pm 90^\circ$ microstrip phase shifter," *IEEE Microw. Wireless Compon. Lett.*, vol. 22, no. 2, pp. 58–60, Feb. 2012.
- [12] P. Sobis, J. Stake, and A. Emrich, "High/low-impedance transmission-line and coupled line filter networks for differential phase shifters," *IET Microw., Antennas Propag.*, vol. 5, no. 4, pp. 386–392, 2011.
- [13] A. Abbosh and M. Bialkowski, "Design of compact directional couplers for UWB applications," *IEEE Trans. Microw. Theory Tech.*, vol. 55, no. 2, pp. 189–194, 2007.
- [14] M. Bialkowski, A. Abbosh, and N. Seman, "Compact microwave six-port vector voltmeters for ultra-wideband applications," *IEEE Trans. Microwave Theory Tech.*, vol. 55, no. 10, pp. 2216–2223, Oct. 2007.
- [15] A. Abbosh and M. Bialkowski, "Design of ultra wideband 3 DB quadrature microstrip/slot coupler," *Microw. Optical Tech. Lett.*, vol. 49, no. 9, pp. 2101–2103, 2007.